THE NIF INJECTION LASER SYSTEM

J. K. Crane *R. B. Wilcox* *M. Hermann* *M. Martinez* *B. Moran*
M. Henesian *G. Dreifuerst* *B. Jones* *J. E. Rothenberg* *K. M. Skulina*
D. Browning *L. A. Hackel* *L. Kot* *F. Penko* *F. Deadrick*

The injection laser system (ILS), or "front end," is the portion of the National Ignition Facility (NIF) where a single pulse is produced, modulated, and shaped, then amplified and multiplexed to feed the 192 main amplifier chains in the NIF.[1] The ILS's three major subsystems are summarized in the overview, then described in detail in their own sections. In many cases, the subsystems have been developed and are in an engineering prototype phase in which we work with outside vendors to produce hardware. We have also connected two of the subsystems, the master oscillator room (MOR) and preamplifier module (PAM) development labs, to perform integrated performance measurements on a combined system.

Overview

The ILS is composed of three major subsystems: the master oscillator room (MOR), the preamplifier modules (PAMs), and the preamplifier beam transport system (PABTS).

The master oscillator room is responsible for generating the single pulse that seeds the entire NIF laser system. In the MOR, this single pulse is phase-modulated to add bandwidth, then multiplexed into 48 separate beamlines on single-mode, polarizing fiber. Before leaving the MOR, the pulses are temporally sculpted into high-contrast shaped pulses designed to produce ignition of the deuterium–tritium (D–T) targets. Forty-eight single-mode fibers from the MOR serve as inputs to the 48 PAMs that are the second major subsystem in the ILS.

The preamplifier modules provide the largest amount of amplification in the entire NIF laser system, >100 dB. In addition to providing amplification, the PAMs spatially shape the Gaussian beam that emerges from the single-mode fiber to form a square beam that is shaped to compensate for the spatial gain profiles of the main slab amplifiers. A third function performed in the PAMs is spectral dispersion of the phase-modulated light produced initially in the MOR. This dispersion is part of a scheme called smoothing by spectral dispersion, or SSD,[2] that reduces the spatial coherence of the laser light irradiating the target. The 48 17-J outputs from the PAMs enter the final subsystem of the ILS, the preamplifier beam transport system.

In the PABTS, the 48 beams from the 48 PAMs are split into 192 separate beams that feed the main amplifier chains. After this four-way split of the beams, each leg has an optical trombone section for precisely adjusting the timing so that all 192 beams converge on target simultaneously.

Figure 1 shows a schematic block diagram of the ILS and its constituent systems. The requirements for the ILS are derived from the overall laser system requirements at the target. Table 1 lists the overall system requirements at the target and the resulting parameters for the ILS determined from the flowdown.

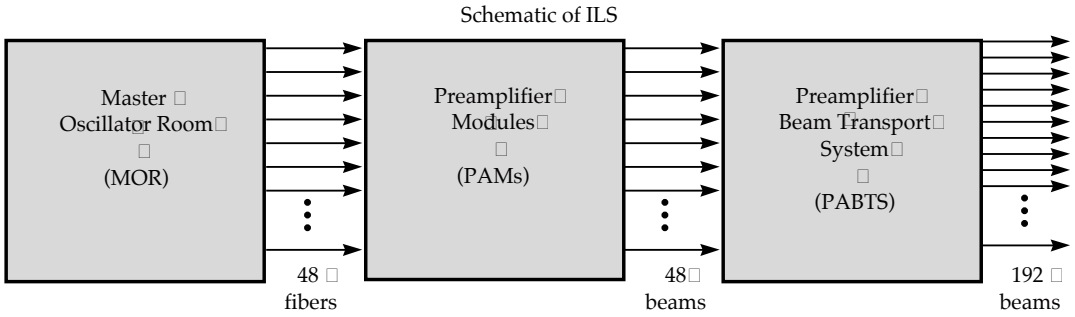

FIGURE 1. The NIF injection laser system (ILS). (70-00-0299-0358pb01)

TABLE 1. System requirements for the laser at the target and the requirements at the output of the ILS, determined from a flowdown of the system requirements back to the front end.

NIF System Requirements[a]		Injection Laser System Requirements	
Output energy	1.8 MJ	Injected energy into main amps	3 J
Peak power	500 TW	Peak power at injection	1.2 GW
Wavelength	352 nm	Preamp output energy (flat-top beam)	22 J
Pulse duration	20 ns	Preamp power energy (shaped beam)	16.9 J
Power balance	8% in 2-ns window	Wavelength	1053 nm
Pointing accuracy @ target	6 μrad	Pulse duration	20 ns
Power dynamic range	>50:1	Output pulse rate	1/20 minute
Prepulse in 20-ns window	$<10^8$ W/cm^2	Prepulse contrast	$>2 \times 10^6$
Number of beamlets	192	Square pulse distortion	<2.3
		Bandwidth	81 GHz
		Critically dispersed (SSD)	–
		Spatially shaped for gain compensation	–
		Number of preamplifier modules	48

[a]Reference 1.

Master Oscillator Room

This section describes the subsystems that make up the MOR. All these systems have been demonstrated at the scientific prototype stage and are being engineered for the final NIF version. A simplified version of the MOR architecture is shown in Figure 2.[3]

The 192 pulses that converge on the target with a combined energy of nearly 2,000,000 J originate as a low-power continuous-wave (CW) signal in the MOR's master oscillator. This oscillator is a fiber distributed feedback (DFB) laser, made by imprinting linear Bragg gratings in an Yb-doped fiber using UV light. This technology is similar to that used in Er-doped fiber lasers for communications.[4] The Bragg gratings define the cavity end reflectors, which are such narrow band reflectors that they allow only one cavity mode to lase.

When pumped with a 120-mW laser diode, the oscillator produces about 50 mW CW in a single longitudinal mode. The master oscillator wavelength is precisely tuned to within 0.01 nm of the desired value by temperature-controlling its mount, which changes the Bragg

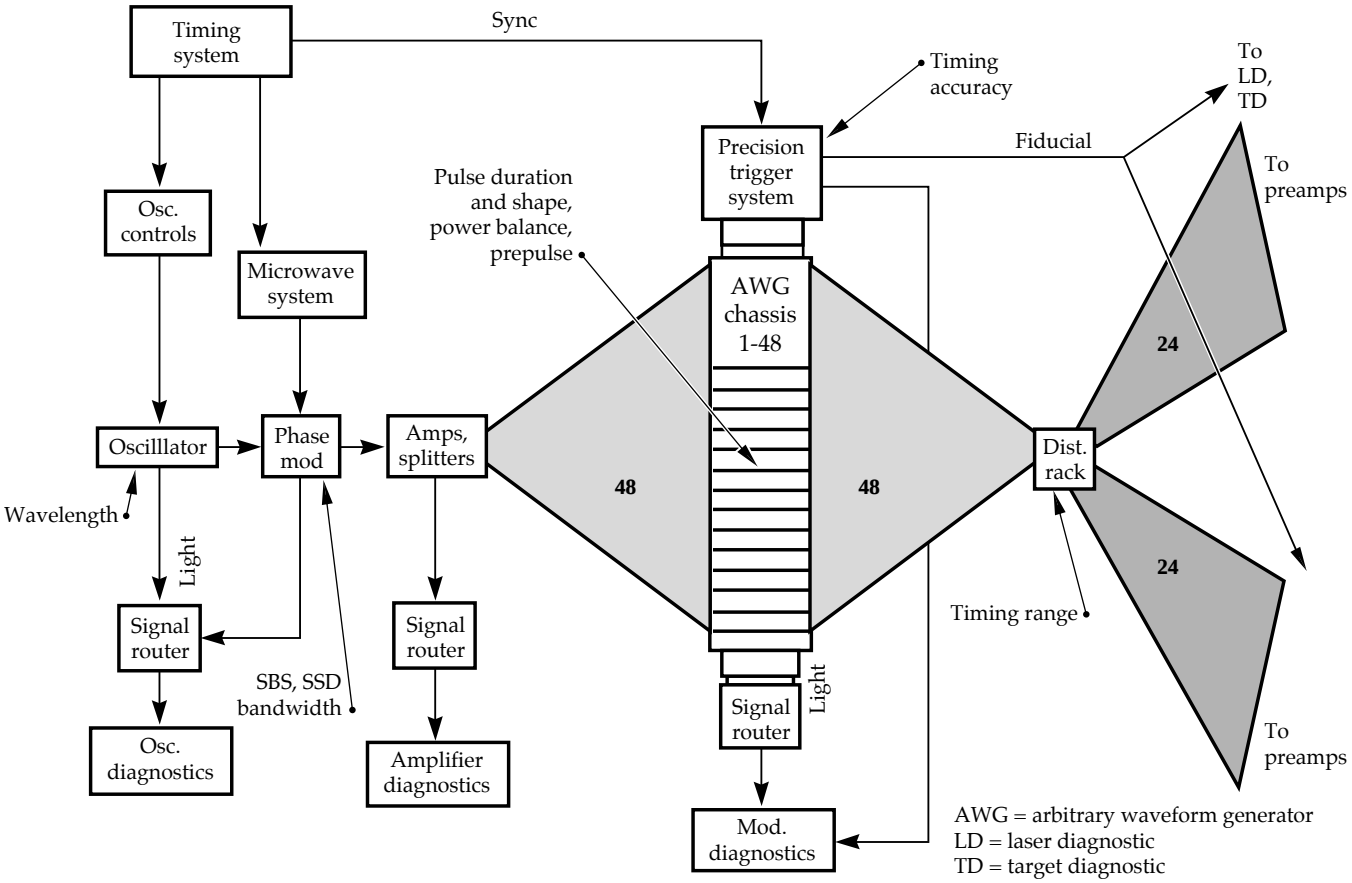

FIGURE 2. The master oscillator room (MOR) architecture. (70-00-0299-0359pb01)

wavelength by strain and the thermooptic effect. Figure 3 shows a picture of a pumped, unmounted oscillator, and a schematic of the fiber master oscillator.

Amplification and Modulation

The CW signal from the oscillator is chopped by an acoustooptic modulator to a pulse width of 100 ns and passed through a double-pass fiber amplifier with a gain of 500. The amplifier is internally filtered to reduce the amount of noise it adds to the oscillator signal. When the signal has passed through the amplifier once, it reflects off a 2-Å-wide passive fiber Bragg grating filter. This reduces amplified spontaneous emission (ASE) noise from the first pass. After a second pass, the output signal is filtered through a 5-nm bandpass filter to further reduce ASE. A directional coupler is used to multipass the amplifier because it has low back reflection, high damage threshold, and nearly the same loss as a circulator at this wavelength. After passing through this amplifier and undergoing several component losses, the 100-ns pulse has a peak power of about 1 W.

At this point, phase modulation is applied to the single-frequency signal to control its eventual interaction with the final NIF optics and the target. Phase modulation at 1.5 GHz produces about 10 optical sidebands, which reduce the spectral intensity in the final optics and prevent stimulated Brillouin scattering (SBS), which could damage the optics.[5] Phase modulation at 17 GHz creates a bandwidth of 3 Å. When diffracted from a grating in the PAM, the 3-Å bandwidth quickly moves the focused laser beam on target to smear out speckle through a process called smoothing by spectral dispersion (SSD).

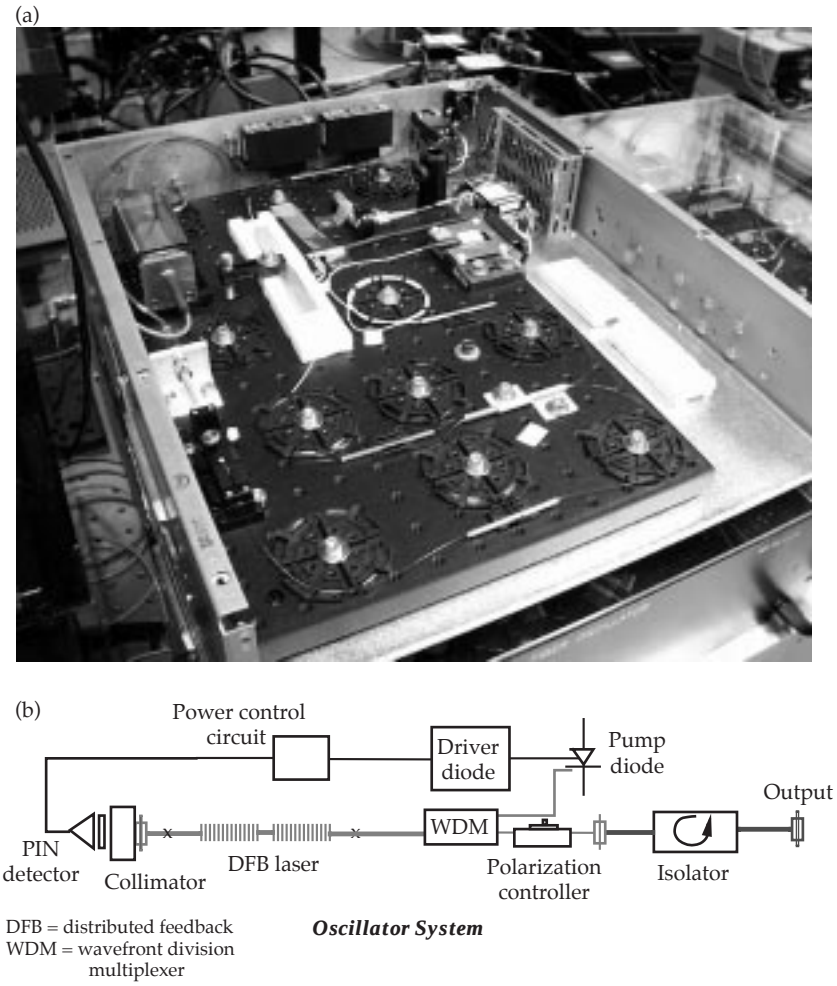

FIGURE 3. (a) Photo of a pumped, unmounted oscillator. (b) Schematic of the fiber master oscillator. (70-00-0599-1058pb01)

Both modulations are applied with lithium niobate, electrooptic waveguide modulators similar to those used in fiber-optic communications. Modulators that produce these modulations require only a few watts of microwave power, reducing the complexity of the drive circuit and enhancing reliability. Because it is important that SBS not damage the NIF optics, a doubly redundant, fail-safe circuit monitors the presence of 1.5-GHz phase modulation and blocks the laser pulse if the amount of modulation is too low. Several parameters are measured on each pulse to ensure that each one has the required bandwidth.

To reduce gain saturation in the fiber amplifiers, the 100-ns pulse is reduced in another waveguide modulator to 30 ns before being introduced into the fiber amplifier and splitter array.

The amplifiers in the array are Yb-doped, two-stage, CW-pumped fiber amplifiers, shown in Figure 4 and developed with JDS Feitel. The first stage is a small core, Yb-doped, gain fiber with gain of 12, followed by a band-stop filter to prevent saturation of the second stage by ASE. The second stage, a power amplifier, is made of larger core fiber and has a gain of 3, for a total gain of 36 for each fiber amplifier. The amplifiers for NIF will be produced to our design and specifications by a commercial manufacturer.

After each stage of amplification, the pulse is split four ways. In the first stage, three outputs are used, so that the total number of outputs in three stages of amplification is $3 \times 4 \times 4 = 48$. The 48 outputs each produce about 2 W in 30 ns.[6]

Arbitrary Waveform Generator

The final temporal pulse shape is sculpted from the 30-ns square pulse after the laser

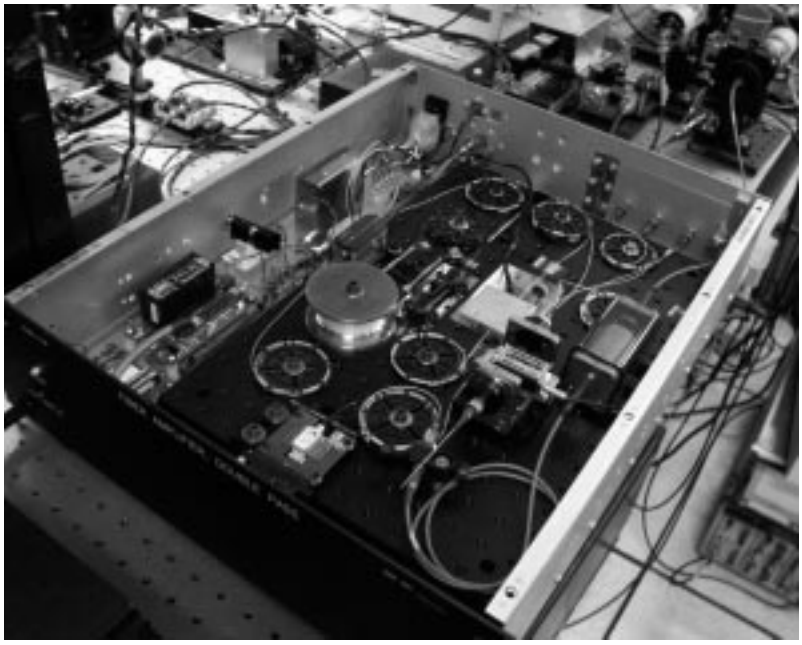

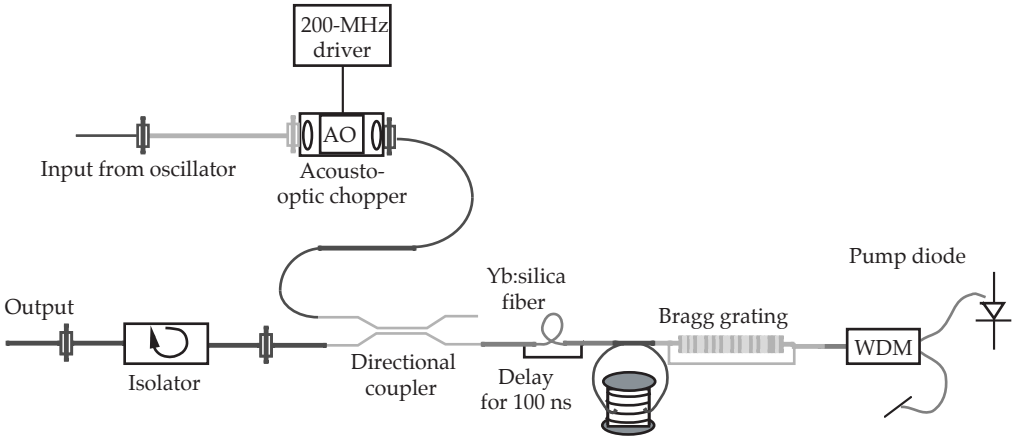

FIGURE 4. The Yb-doped, two-stage, CW-pumped fiber amplifiers in the splitter array. (70-00-0599-1059pb01)

has fanned out to 48 parallel fiber lines. Together with Highland Technology, we developed a high-bandwidth, programmable, arbitrary waveform generator (AWG) to produce the high-temporal-contrast pulses that are needed for fusion ignition.[7]

An electronic waveform generator supplies a shaped-voltage pulse to an integrated optic, lithium niobate amplitude modulator, which modulates the light pulse. The electronic waveform generator works by adding 300-ps voltage pulses separated in time by 250 ps. NIF will have 96 300-ps pulse generators, each of which can be precisely controlled in amplitude. By programming these pulse amplitudes, we can create an arbitrary pulse shape.

There are some applications where a shorter pulse is required. This is provided by a second pulse generator through a special circuit. For example, some targets employ a secondary target that is illuminated by a short laser pulse. When the pulse strikes the target, x rays are produced. These x rays act like a photo flash to capture an instant in the target implosion. Also, timing of the 192 beams to coincide in the center of the target chamber requires a short pulse for timing precision. In these cases, a pulse of about 150 ps is produced.

The electronic waveform generator and optical modulator are combined in a single chassis that is being produced by an outside manufacturer. There will be 48 of these units in the final NIF laser system. Figure 5a shows the generator.

Figure 5b shows a typical, high-temporal-contrast pulse generated by the AWG. It is essential that these pulses arrive at the target simultaneously to provide uniform target implosion. Only 12 ps of timing uncertainty is allowed for the pulses leaving the MOR.

Synchronization of the pulse generators is accomplished by triggering each one with a short optical pulse passively split from a single, high-energy optical pulse. In this trigger system, a 100-ps electrical pulse synchronized with the integrated timing system (ITS) drives an electrooptic modulator to produce a 100-ps optical pulse. This is amplified in fiber amplifiers and split to trigger the pulse waveform generators. A portion of this pulse is also sent out of the MOR to fiducial laser and target diagnostic systems to be used as a timing marker exactly synchronized with the main optical pulses.

After final temporal shaping, the 48 parallel fiber lines are routed through a central distribution rack. From there they are sent to the 48 PAMs. The central fiber distribution is carefully designed to ensure that the individual lines produce the correct timing delay to each PAM.

We can add or subtract fiber jumpers to discretely vary the delay of each beamline for needed adjustment, or to satisfy the requirements of special experiments. In addition to the laser itself, the MOR contains auxiliary systems for controls, diagnostics, and precision timing.

Preamplifier Modules

As part of the development effort for the ILS, the various subsystems in the MOR and PAM were assembled and tested in the laboratory, and then combined into an Integrated ILS testbed.[8] Using this combined system, we were able to test those specifications of the ILS that required the functions of both the MOR and PAM.

Each of the 48 fibers from the MOR distribution rack feeds one of the 48 PAMs in the NIF laser system. The PAM is a high-gain (>100 dB) preamplifier that also spatially shapes the beam for the main amplifier chain. Figure 6 is a schematic of the PAM showing the three major subsystems: an ultrastable, high-gain, diode-laser-pumped, Nd:glass regenerative amplifier; a beam-shaping module; and a four-pass amplifier.

(a)

(b)

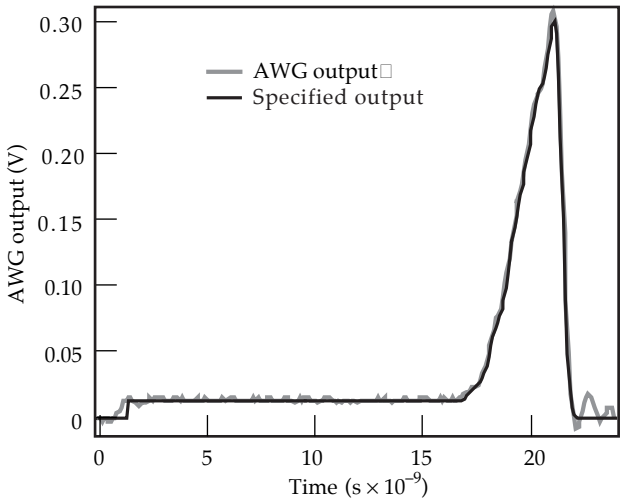

FIGURE 5. (a) The arbitrary waveform generator (AWG) chassis. (b) Plot showing specified (black) and measured (gray) electronic pulse shapes produced by the AWG. (70-00-0299-0360pb01)

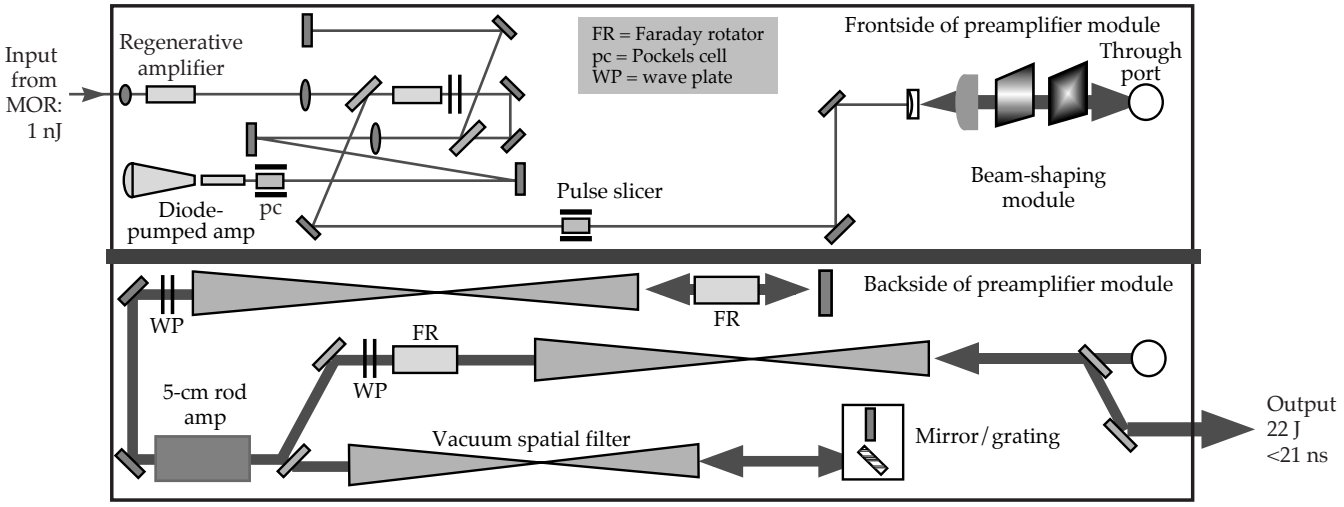

FIGURE 6. Optical layout of the preamplifier module (PAM). (70-00-0299-0361pb01)

Regenerative Amplifier

The regenerative amplifier is the highest gain amplifier in the entire NIF laser chain.[9–11] The optical layout for the regenerative amplifier, or "regen" for short, is shown in Figure 6. The input section to the regen consists of a fiber launch, where the pulse from the MOR is launched from single-mode fiber into free-space via a precision fiber positioner and a short-focal-length lens. Next, two Faraday isolators in series protect the single-mode fiber from a high-intensity pulse reflecting, or propagating back, from the regen output. A second lens, in conjunction with the short-focal-length lens in the fiber launch, forms a telescope to match the beam size at the fiber output to the laser cavity mode for efficient coupling of energy into the regen.

A Faraday rotator, a half-wave plate (WP), and a thin-film-polarizer (TFP) form a unidirectional coupler to separate the counterpropagating input and output laser pulses. The input laser pulse from the MOR is injected into the regen cavity through a second TFP.

The regen cavity is a long, asymmetric cavity with a single, diode-laser-pumped, Nd:glass amplifier located at one end. The amplifier has a single-pass gain of $G = 1.4$ in a 5-mm diameter × 50-mm rod that is end-pumped by a 4-kW diode array. The cavity transmission is $T = 0.77$, so the net gain per round trip of the regen is $G_{net} = G^2 \cdot T = 1.5$. A cavity Pockels cell switches polarization of the input pulse after it has made a single pass, trapping the pulse in the regen until the Pockels cell is switched back to its original polarization.

Each time the circulating pulse makes a round trip in the cavity, the pulse is amplified by G_{net}. The total gain of the regenerative amplifier is the net gain raised to the power of the number of round trips that the pulse makes in the cavity before being switched out. For example, if the number of round trips in the regen cavity is $k = 40$, then the total regen gain is

$$G_{total} = (G_{net})^k = (1.50)^{40} = 1.4 \times 10^7 \quad . \qquad (1)$$

Eventually the amount of extracted energy depletes the available stored energy in the amplifier (amplifier saturation) and the net gain drops below unity. In typical operation we extract 12 mJ from the regen for 0.8-nJ input, for a total gain of 72 dB. Upon leaving the regen cavity, the amplified pulse passes through a second Pockels cell called the slicer, which acts as an optical gate. The slicer passes the main regen pulse while rejecting pre- and postpulses that leak out of the cavity due to imperfect polarization switching.

The output mode from the regen is a 3.5-mm-diam circular Gaussian-shaped beam.

Beam-Shaping Module

The next subsystem in the PAM is the beam-shaping module, where the round Gaussian beam is converted to a square-shaped beam that is sculpted in a well defined manner to precompensate for the spatial gain profile of the main amplifiers.[12] The goal is to produce a spatially flat-top beam at the NIF target chamber to yield the maximum irradiance at the target.

First the round beam is magnified by a 20× telescope. The expanded Gaussian beam is shaped by an anti-Gaussian filter that flattens the center of the beam. This truncated Gaussian beam is further shaped by a gain-compensating mask that carves out the center of the beam to produce the final shape. We determine this final shape based on a complex diffraction code that models an entire beamline, including the spatial gain profiles of the main amplifiers.[12] The final mask in the beam-shaping module, a serrated aperture, apodizes the beam so that it will propagate over a long distance with minimal ringing at the edges of the beam from diffraction.[13]

All of the beam-shaping masks in the module are made by depositing chrome on glass in a standard photolithographic process. The shaping masks reduce the energy from the regen by a factor of 10 to 15, from 12 mJ down to <1 mJ. This spatially shaped beam is injected into the final PAM system, the four-pass amplifier.

Four-Pass Amplifier

The final amplifier in the PAM is laid out in a four-pass configuration as shown in Figure 6. The input beam is spatially filtered by a vacuum relay telescope with a pinhole that blocks the higher spatial frequencies produced by the high-frequency teeth in the final apodizing mask. The filtered input beam passes through a combination of Faraday rotator, half-wave plate, and thin-film polarizer that acts as a directional coupler to separate the input beam from the counterpropagating output beam exiting from the four-pass cavity.

The four-pass cavity contains a Nova, 5-cm, flashlamp-pumped, rod amplifier at the cavity center. This amplifier can operate with a single-pass gain of 20.

Due to the high, single-pass gain of the 5-cm amplifier, the cavity is especially susceptible to unwanted, parasitic oscillation. Parasitic oscillation can occur in a high-gain amplifier if there is sufficient gain and feedback to cause oscillation. This oscillation is uncontrolled and chaotic and produces a background of intense light that can propagate into the main amplifier chain along with the amplified and formatted pulse from the MOR.

We take several steps to successfully eliminate unwanted oscillation in the four-pass cavity. These include carefully controlling the polarization of the light using the Faraday rotator and the quarter-wave plate, and offsetting the beam slightly from the optical axis as it propagates through the cavity so light is never reflected directly back on itself.[14]

Figure 7 shows the measured output energy of the four-pass amplifier as a function of energy at the input. The solid curve in the plot is the predicted performance based upon a Frantz–Nodvik model for saturated gain.[15] The dashed line shows the required performance of the four-pass amplifier for an unshaped input pulse (see Table 1).

A second function of the four-pass amplifier optical layout is to provide angular dispersion of the light that has been frequency modulated in the MOR for SSD. To achieve this, we replace one of the end mirrors in the four-pass cavity with a diffraction grating positioned at the Littrow angle so the first diffraction order is reflected back in the same direction as the incoming beam. If the four-pass output is viewed in the far field (i.e., at the focus of a lens), the focal spot is dithered in one dimension at the sinusoidal frequency of the rf driver to the modulator (e.g., 17 GHz). The angularly deflected light from the amplifier propagates through the rest of the amplifier chain to the target chamber and final optics assembly, where it passes through a special phase plate.

The combination of the rapid dithering of the FM light due to dispersion from the grating, and the smearing of the focal spot

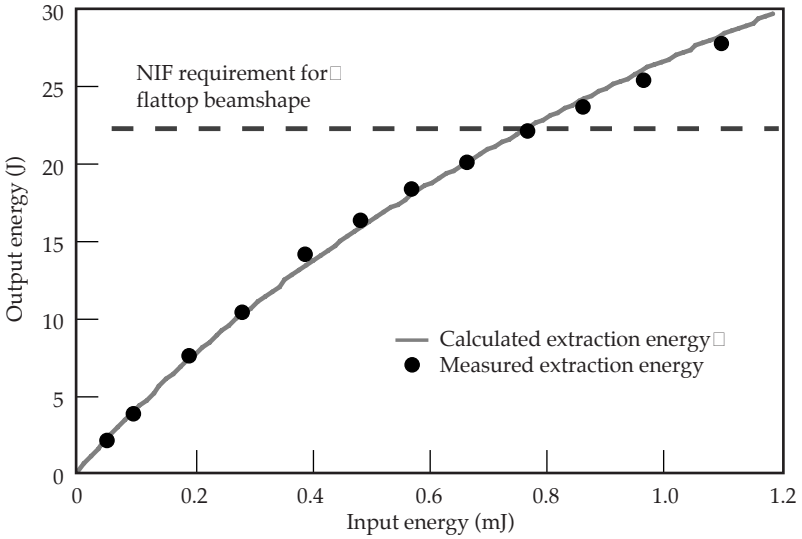

FIGURE 7. PAM output energy as a function of four-pass input energy. Solid curve is a Frantz–Nodvik model for saturated gain. (70-00-0299-0362pb01)

produced by the random phase plate, reduces the spatial coherence (or speckle pattern) normally associated with coherent light and increases the uniformity of the target illumination.

The current beam-smoothing requirement for the NIF is a 3-Å bandwidth, critically dispersed in one dimension (see Table 1). "Critically dispersed" means that the temporal skew produced across the 3-cm beam by the grating at Littrow angle must be equal to the period of the sinusoidal rf waveform that drives the phase modulator. The temporal skew ΔT is given by

$$\Delta T = 2D\tan\theta_L / c = 1/f_{mod}\,, \qquad (2)$$

where $D = 30$ mm is the beam dimension at the grating in the dispersion direction, and f_{mod} is the rf driver frequency. The Littrow angle is given by $\theta_L = \sin^{-1}(\lambda/2d)$, where λ is the wavelength of the laser and d is the grating groove spacing.

In the current design, the modulation frequency for SSD is 17 GHz, and the critical dispersion requirement is slightly exceeded for a 600-line/mm grating. The 17-GHz modulator system was not available for the ILS subsystem tests, so we used a 3-GHz modulation frequency. We used an 1800-line/mm grating that exceeded the critical dispersion requirement and allowed us to clearly resolve individual FM sidebands.

Figure 8a is an image taken by the far-field camera diagnostic at the output of the four-pass amplifier. The angular dispersion produced by the 1800-line/mm grating cleanly separates the individual spots in the far field. We show a plot in Figure 8b comparing a lineout from the camera image with a power spectrum for an 81-GHz modulation bandwidth. The power spectrum, $P(t)$, is given by the Bessel series:

$$E(f) \approx \sum_{n=0}^{\infty} J_n(m)\bullet[\delta(f_0 + nf_{rf}) + (-1)^n\,\delta(f_0 - nf_{rf})] \qquad (3)$$

$$P(f) \approx |E|^2\,, \qquad (4)$$

where $E(f)$ is the laser field in the frequency domain, J_n is the nth order Bessel function, m is the modulation index, δ is the delta function, and f_{rf} is the rf frequency driving the phase modulator. The locations of the peaks and their magnitudes from the image lineout accurately compare with the simulated spectral peaks. The 81-GHz FM spectrum is confirmed by the spectrometer measurements in the MOR and at the regen output.

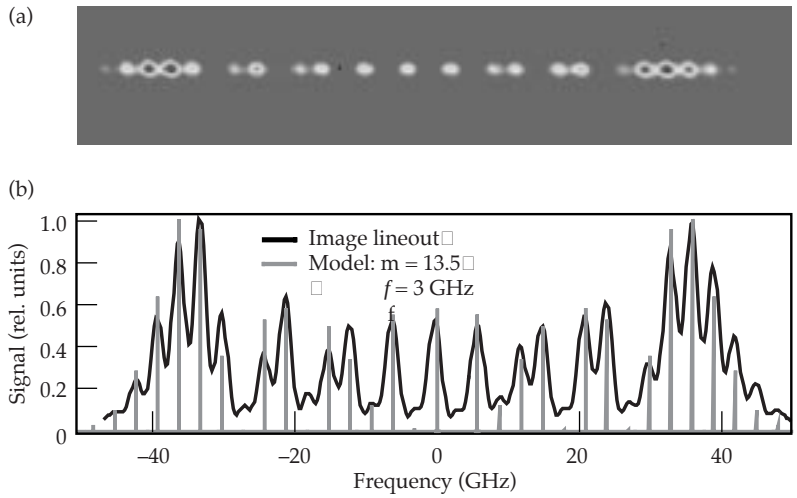

FIGURE 8. (a) The far-field camera image at the PAM output showing the beam dispersed by an 1800-line/mm grating. (b) Plot comparing a horizontal lineout from (a) and an FM spectrum where the rf frequency is 3 GHz and the modulation depth is 13.5. (70-00-0299-0363pb01)

The results from experiments on the Integrated ILS Testbed demonstrate that the PAM and MOR combined systems meet the requirements listed in Table 1. The optical layout and specifications demonstrated in the PAM development lab become the basis for the first PAM engineering prototype.

PAM Engineering Prototype

The 48 preamplifier modules that seed the main amplifier chains in the NIF laser system reside on the preamplifier support structure (PASS), a large space frame in the main laser bay. The PAMs are designed to be line-replaceable units, or LRUs, that can slide into place on precision rails on the PASS or be quickly removed as a self-contained unit and replaced or repaired as needed.

In our laboratory we set up and assembled the first preamplifier module, an engineering prototype of the production PAMs that will form part of the ILS. Figure 9 is a photograph of the PAM prototype. We reproduced the three optical subsystems, the regenerative amplifier, the beam-shaping module, and the four-pass amplifier that were developed and demonstrated on the Integrated ILS testbed, and mounted these subsystems on the PAM prototype. The regenerative amplifier and beam-shaping module are mounted on one side of a vertical optical support structure. The larger four-pass amplifier is mounted on the opposite side.

The electronics to support the PAM include: a diode-laser power supply, stepper motor controllers, ion-pump controllers, timing modules, temperature controllers, and a VME-based embedded processor controller that provides overall electronics control of the PAM. These electronics units are mounted above the optics support structure in an electronics bay that runs the length of the PAM. A high-energy, electrical pulser that drives the six flashlamps in the 5-cm rod amplifier is housed in a separate unit, apart from the PAM.

We have operated the PAM prototype over the past several months to demonstrate the requirements listed in Table 1. In addition, we developed a high-resolution output beam diagnostic to accurately measure the wavefront, near-field contrast, and the far-field spot size at the output of the PAM prototype. Figure 10 shows processed data taken with the high-resolution out-put beam diagnostic for a 17-J shot. The information that we garner from these comprehensive tests of the PAM engineering prototype will enable us to design the 48 production PAMs.

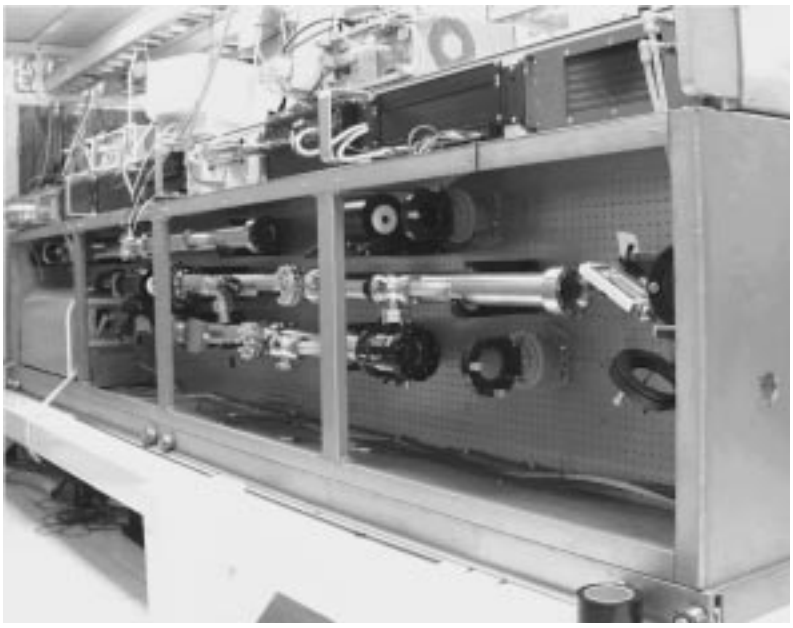

FIGURE 9. PAM engineering prototype mounted on mini-PASS structure. This view shows the four-pass amplifier.
(70-00-0299-0364pb01)

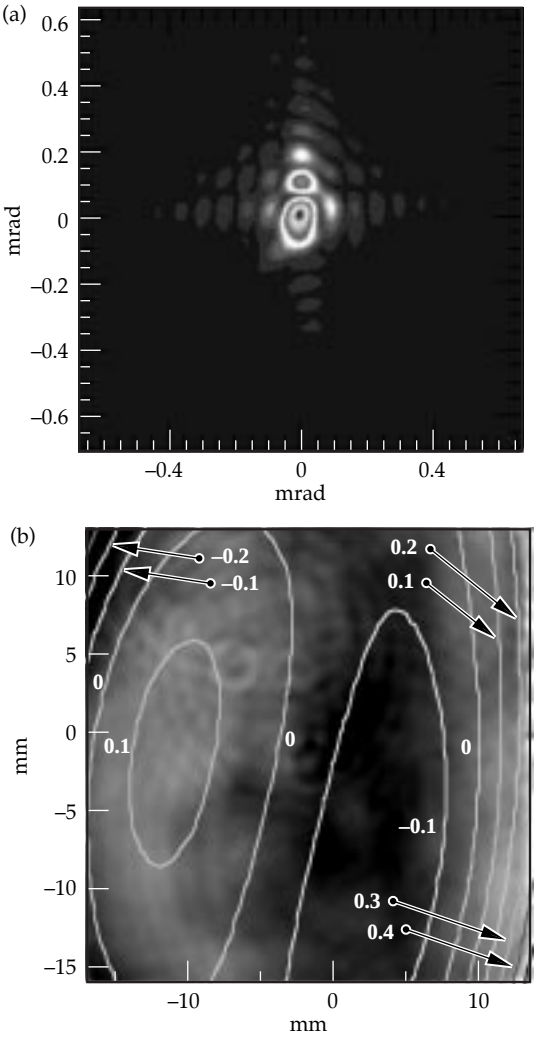

FIGURE 10. (a) Far-field image at the output of the PAM prototype taken with a high-resolution PAM output diagnostic (Strehl ratio = 0.65). (b) Phase map of the output wavefront taken with a radial shearing interferometer (peak-to-valley phase = 0.71λ).
(70-00-0299-0365pb01)

Preamplifier Beam Transport System

The final system in the ILS, or front end, of the NIF laser is the PABTS, shown in Figure 11. The 16.9-J output from a PAM passes through an isolation module that contains a large-aperture Faraday rotator, half-wave plate, and polarizers to isolate and protect the front end from a high-energy pulse traveling backwards from the main amplifier chain.

From the isolation module, the beam enters the 1:4 split assembly, where the single beam is split into four beams that will seed four separate main amplifier chains. The four-way split and balancing of power among the four legs is accomplished using thin-film polarizers and half-wave plates.

Each of the beams passes through a six-element vacuum relay telescope that relays the beam to the input relay plane of the transport spatial filter. This zoom telescope has variable magnification from 0.95 to 1.02 and can be used to adjust the size of the beam in each of the four legs to accommodate changes in the main amplifier's optics.

Next a timing section allows for adjustment of the timing in each leg by changing the optical path length via a translating mirror. A pair of turning mirrors directs the beam either into the transport spatial filter (TSF), or a final telescope prior to the TSF, depending upon the side of the laser space frame in relation to the main amplifiers.

Detailed mechanical and optical designs of the PABTS are complete, and hardware prototyping is under way. One quad of a PABTS beamline will be built in 1999.

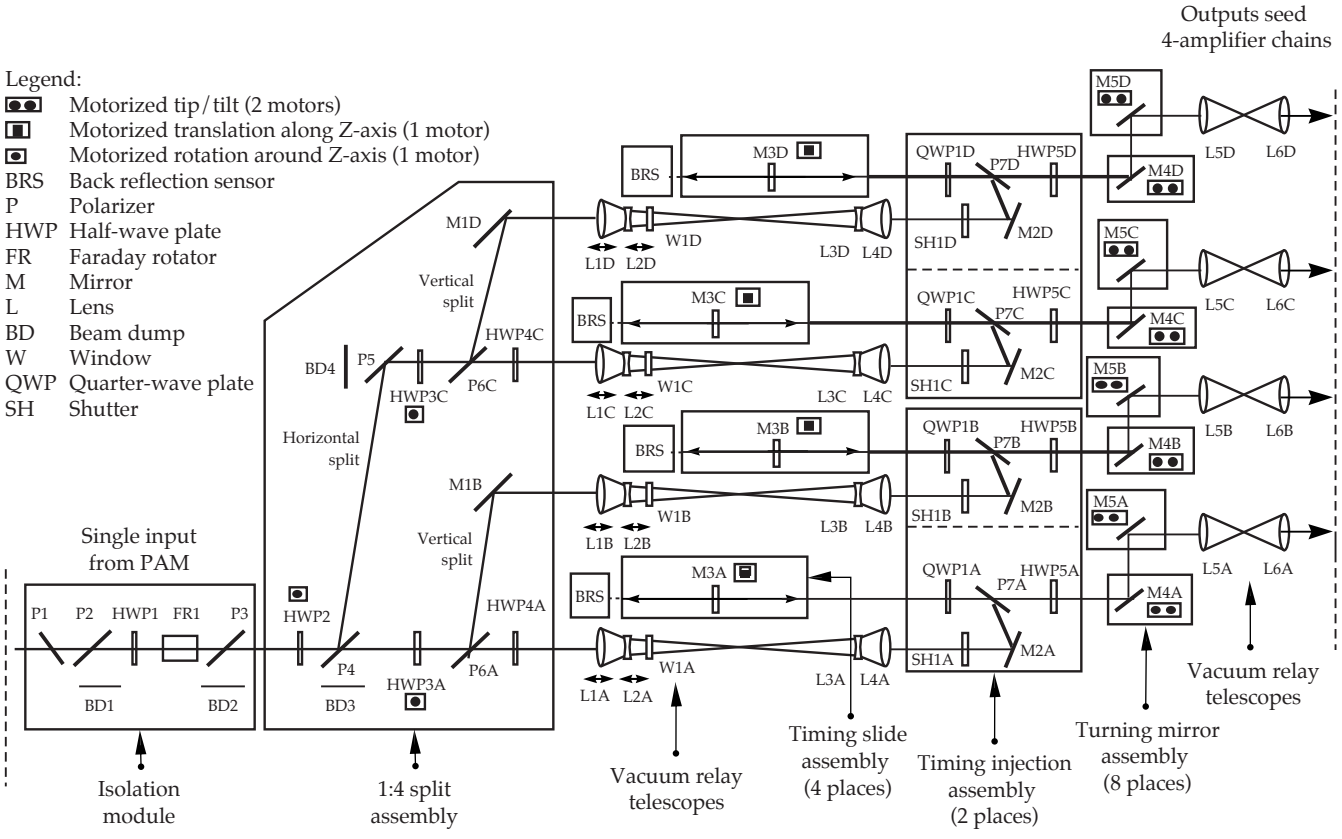

FIGURE 11. The preamplifier beam transport system (PABTS); different subassemblies are designed to be line-replaceable units. (70-00-0299-0366pb01)

Summary

The ILS, or front end, of the NIF laser system is nearing the end of its development phase. In the past year, we performed a series of experiments that demonstrated or exceeded the performance specifications listed in Table 1 for the combined MOR and preamplifier development systems. Many of the subsystems described in this article and demonstrated in our development laboratories are now engineering prototypes. In the coming year, we will assemble an engineering prototype of the entire ILS, including MOR, PAM, and PABTS, plus the computer controls, timing, and diagnostics systems. We will then demonstrate the integrated operation and performance of the NIF laser system front end.

Acknowledgments

We thank the important contributions made by several people in various key stages of the ILS development: Ray Beach, Scott Burkhart, Scott Mitchell, Mike Perry, Jim Davin, Brent Dane, Ralph Page, and Nick Hopps.* In addition we would like to acknowledge the scientific, technical, and design contributions of the following people: Richard Hackel, Ernesto Padilla, Ernie Dragon, Rod Lanning, Regula Fluck, Dave Young, Jim Crawford, Rob Campbell, John Braucht, Ron Tilley, Marcus Bartlow, Pete Ludwigsen, Mike Gorvad, Curt Laumann, Dave Wang, Dave Aikens, Bob Powers, Horst Bissinger, Steve Herman, Russ Jones, Brad Golick, Don Bartel, Jim Hauck, Ron Korniski, Gloria Zuleta, Don Fleming, Greg Fischer, M. Reta, Kathy Coatney, Will House, Annette Springer, Cidelia Sanchez, Lori Dempsey, and Frances Mendieta.

*Atomic Weapons Establishment, Aldermaston, Berkshire, UK

Notes and References

1. J. A. Paisner, J. D. Boyes, S. A. Kumpan, W. H. Lowdermilk, and M. Sorem, "Conceptual Design of the National Ignition Facility," *Proceedings of the First International Conference on Solid State Lasers for Application to Inertial Confinement Fusion*, Monterey, CA, May 31–June 2, 1995, *SPIE Proceedings Series* **2633**, 2.
2. S. Skupsky et al., *J. Appl. Phys.* **66**, 3456–3462 (1989).
3. R. B. Wilcox, D. Browning, G. Dreifuerst, E. Padilla, and Frank Penko, "Development System Performance of the NIF Master Oscillator and Pulse-Forming Network," *Third International Conference on Solid State Lasers for Application to Inertial Confinement Fusion*, Monterey, CA, June 1998.
4. A. Asseh et al., *Electronics Letters* **31**(12) 969 (1995).
5. J. R. Murray et al., *J. Opt. Soc. Am. B* **6**, 2402–2411 (1989).
6. R .B. Wilcox, D. F. Browning, and R. H. Page, "Fiber DFB Lasers as Oscillators for High-Power MOPA Systems," *Conference on Lasers and Electrooptics (CLEO)*, Baltimore, MD (1999).
7. S. C. Burkhart, R. B. Wilcox, D. Browning, and F. Penko, "Amplitude and Phase Modulation with Waveguide Optics," *Proceedings of the Second International Conference on Solid State Lasers for Applications to Inertial Confinement Fusion*, Paris, France, Oct. 22–25, 1996, *SPIE Proceedings Series* **3047**, 610–617.
8. J. K. Crane et al., "Integrated Operations of the National Ignition Facility (NIF) Optical Pulse Generation Development System," *Third International Conference on Solid State Lasers for Application to Inertial Confinement Fusion*, Monterey, CA, UCRL-JC-129871 (June 1998).
9. J. K. Crane et al., *ICF Annual Report 1997*, Lawrence Livermore National Laboratory, Livermore, CA, UCRL-LR-105821-97, 246–259, (1998).
10. M. D. Martinez et al., "Optimized, Diode-Pumped, Nd:Glass, Prototype Regenerative Amplifier for the National Ignition Facility," *Proceedings on Optoelectronics and High-Power Lasers & Applications*, San Jose, CA, Jan. 24–30, 1998, *SPIE Proceedings Series*, vol. 3267, pp. 234–242.
11. N. W. Hopps et al., "Optimization of the Alignment Sensitivity and Energy Stability of the NIF Regenerative Amplifier," *Third International Conference on Solid State Lasers for Application to Inertial Confinement Fusion*, Monterey, CA, UCRL-JC-130961 (June 1998).
12. M. Henesian et al., " Diffraction Modeling of the National Ignition Facility (NIF) Optical Pulse Generation System and Integration into the End-to-End System Model," *Third International Conference on Solid State Lasers for Application to Inertial Confinement Fusion*, Monterey, CA (June 1998).
13. J. M. Auerbach and V. P. Karpenko, *Applied Optics* **33**, 3179–3183 (1994).
14. B. D. Moran et al., "Suppression of Parasitics and Pencil Beams in the High-Gain National Ignition Facility Multipass Preamplifier," *Proceedings on Optoelectronics and High-Power Lasers & Applications*, San Jose, CA, Jan. 24–30, 1998, *SPIE Proceedings Series*, vol. 3264 , pp. 56–64.
15. L. M. Frantz and J. S. Nodvik, *J. Appl. Phys.* **34**, 2346–2349 (1963).